Gelation Mechanism Revealed in Organometallic Gels: Prevalence of van der Waals Interactions on Oligomerization by Coordination Chemistry

Yinping Wang, Yannick Coppel, Juliette Fitremann, Stéphane Massou, Christophe Mingotaud, Myrtil Kahn

Gelation Mechanism Revealed in Organometallic Gels: Prevalence of van der Waals Interactions on Oligomerization by Coordination Chemistry

Yinping Wang,[a,b] Yannick Coppel,[a] Juliette Fitremann,[b] Stéphane Massou,[a] Christophe Mingotaud,*[b] and Myrtil L. Kahn[a]*

[a] Y. Wang, Dr. S. Massou, Dr Y. Coppel, Dr. M. L. Kahn
Laboratoire de Chimie de Coordination, CNRS, UPR-8241,
205 route de Narbonne, 31077 Toulouse Cedex 04, France
E-mail: myrtil.kahn@lcc-toulouse.fr

[b] J. Fitremann, C. Mingotaud
Laboratoire des IMRCP, Université de Toulouse, CNRS UMR 5623
Université Toulouse III – Paul Sabatier
118 route de Narbonne 31062, Toulouse Cedex 9, France
E-mail: christophe.mingotaud@univ-tlse3.fr

Supporting information for this article is given via a link at the end of the document.

Abstract

Shaping of nanomaterials is a necessary step for their inclusion in electronic devices and batteries. For this purpose, the formulation of a moldable material including these nanomaterials is desirable. Organomineral gels are a very interesting option, since the components of the nanomaterial itself form a gel without the help of a binder. As a consequence, the properties of the nanomaterial are not diluted by the binder. In this article we studied organometallic gels based on a [$ZnCy_2$] organometallic precursor and a primary alkyl amine which together forms spontaneously gels after few hours. We identified the main parameters controlling the gel properties monitored by rheology and NMR measurements. The experiments demonstrate that the gelation time depends on the length of the alkyl chain of the amine and that the gelation mechanism derived firstly from the rigidification of the aliphatic chains of the amine, which takes precedence over the oligomerization of the inorganic backbone. This result highlights that the control of the rheological properties of organometallic gels remains mainly governed by the choice of the amine.

Introduction

In the past decades, research in nanoscience has created numerous chemical or physical pathways leading to innovative inorganic materials [1]. A large number of studies dealing with the controlled synthesis of nanomaterials focused on identifying the experimental parameters controlling the final size and shape of the nanomaterials for which many interesting properties for their application are related. For metal oxides, this is particularly true for their used in electronic, optics or chemistry [2]. Organizing these nano-objects on a larger scale or even shaping the final material at the macroscopic level is also necessary to get functional devices. This challenge has stimulated the development of several shaping methods leading to thin films, porous or 3D organized materials, all of which are often easier to obtain when a gel with controlled rheological properties is used [3]. It explains why the "sol-gel" method which is based on the use of aqueous solutions of metal alkoxides or metal salts in which a controlled hydrolysis and condensation process is triggered, leading to metal oxides, is so popular [4]. For some metals, the hydrolysis equilibrium is however not favorable. In that case, the Pechini method (or polymerizable complex method) which is based on the polyesterification of metal-citrate complexes that leads to the formation of an extended covalent network, was developed [5]. These two methods are however restricted to aqueous systems. Non-aqueous [6] sol–gel routes were also developed using metal salts such as metal halides, metal alkoxides, metal acetates or metal acetylacetonates. These ways proceed without external addition of water [7] but the reactions are, especially for transition metal alkoxides, very fast and hard to control, leading to amorphous gels [8]. Therefore, the final aerogels or xerogels have to be thermally treated to induce crystallization of the metal oxide framework. In addition, the number of suitable molecular precursors is still limited. Fortunately, we have recently described the use of organometallic precursors such as alkyl zinc, in the presence of ligands such as alkyl amines, as a powerful alternative for preparation of gels [9]. This organometallic pathway was successively applied to several metal elements. Each time, mixing fatty amines with organometallic compounds induces the formation of oligomeric structures between metallic centers. The corresponding organometallic gels can therefore be considered as an emerging class of gels where metal ions or metal particles are necessary bricks for the formation of the gel network [10]. This kind of gels can be used as sensors [9, 11] as stationary phase for extractions [11, 12] and for catalysis [12,13]. They are also studied for their electronic or electrochemical properties [14]. Also, thanks to their viscoelastic properties, they enable the easy shaping of organometallic species, notably molding, extrusion and 3D printing [9]. These gels were obtained using dodecylamine (hereafter DDA) in a 1/2 Zn/amine ratio [15]. Interestingly, gel formation was not observed previously when hyper-branched amines or secondary amines were used [16]. For a given metal (e.g. zinc), understanding the effect of the molecular structure of the amine on the gelation is important but up to now unreported.

Here, we describe the effect of the aliphatic chain length on the formation of processable zinc organometallic gels using NMR spectroscopy, which has been previously successfully used to study in-situ processes that evolve with time [17]. These results were confirmed by rheological measurements for the longest aliphatic chains and highlighted the advantages of using NMR spectroscopy for characterizing these air sensitive gels. Furthermore, the NMR spectroscopic studies gave us reliable information how the gelation takes place at molecular scale.

Results and Discussion

The organometallic gels were obtained by mixing the zinc precursor, dicyclohexyl zinc (hereafter [Zn(Cy)$_2$]) with two equivalents of amines (1:2) of various alkyl chain length (from pentyl, C5 to dodecyl, C12, Scheme 1). To characterize the gelation process, two methods were implemented. First, the viscoelastic properties of the mixtures have been monitored with a rheometer under nitrogen flow. Secondly, NMR spectroscopy studies were performed to monitor the changes at the molecular level. Vial inversion tests were also performed to observe directly the gel formation.

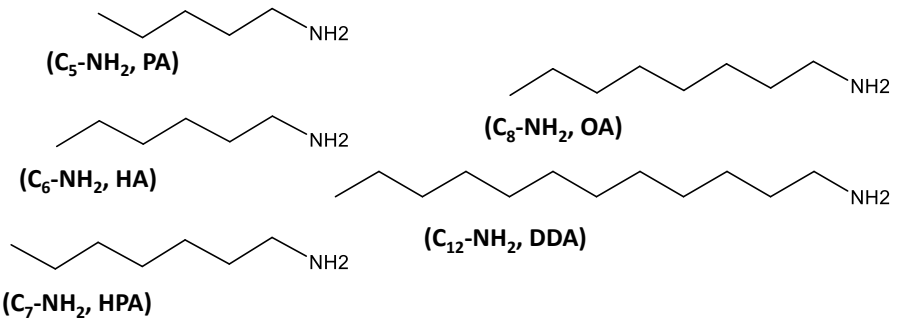

Scheme 1: Amines of various alkyl chain length used in this study from pentyl to dodecyl.

Regardless of the amine backbone, mixing with the zinc precursor leads to (i) the formation of a 1/1 adduct between the zinc precursor and the amine (Scheme 2a), (ii) the conversion of this adduct into an amido cyclohexyl zinc complex through an intramolecular acid−base reaction with release of cyclohexane (Scheme 2b), and (iii) the dimerization of the amido cyclohexyl zinc complex via dative bonding leading to amido dicyclohexyl zinc oligomers of increasing size via a polycondensation reaction (Scheme 2c). One can therefore envisione that gel forms from the entanglement of the resulting oligomers and/or of the aliphatic chains of the amines.

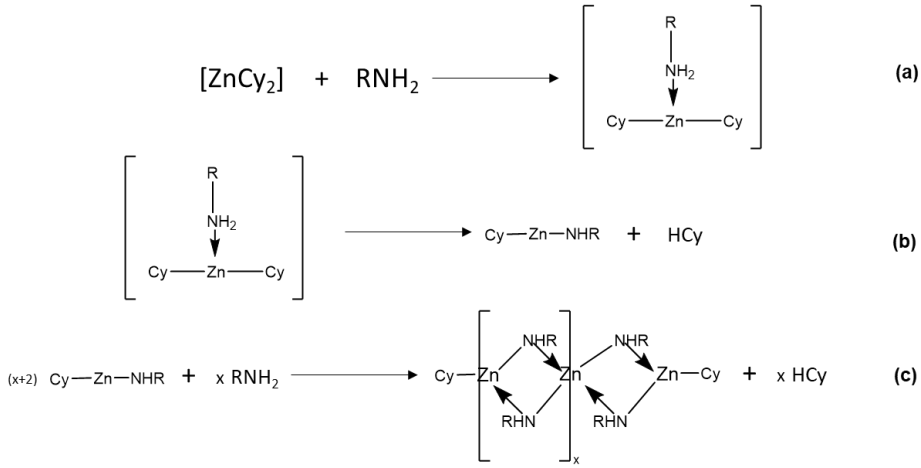

Scheme 2: Reactions leading to oligomers.

Rheology. To set up the rheological measurements, two requirements which represent experimental difficulties had to be overcome. The first one is that the measurement had to be performed under inert atmosphere so that the hydrolysis of the mixture was avoided or highly reduced. Since the rheometer is not a tightly closed system, to the contrary of a glove box and/or NMR rotors, a slow nitrogen flow

was maintained during the whole measurement. This gaseous flow did not flush out significantly the amines of high boiling point (octylamine: b.p. = 176°C or dodecylamine, b.p. = 259 °C). But for shorter alkyl chain amines (e.g. hexylamine), even when the flow is set up at a minimum to avoid hydrolysis, part of the amine is evaporated, leading to changes in the mixture proportions. Rheological measurements thus reflected both stoichiometric modifications and effects of the gelation. The second difficulty to monitor the gelation by rheology is the fact that the moduli increased from c.a. 0.1 Pa to c.a. 10000 Pa, that is, 5 orders of magnitude. The applied stress must be adapted throughout the experiment to keep a good sensitivity. But if a brutal increase of the applied stress is applied, the sample breaks. Thus, stepwise and delicate increase of the stress must be applied. Even by applying these two constraints, avoiding hydrolysis and breakage was not granted all the time, making the measurement cumbersome.

Figure 1 shows the rheogram for the $[Zn(Cy)_2]$/octylamine (OA) mixture. Up to 3h40 after injection in the rheometer (i.e. 7h40 min after mixing the amine and the zinc precursor), both moduli are still low (viscous modulus G'' ≈ 0.25 Pa; elastic modulus G' ≈ 0.15 Pa) with G'' larger than G', which is characteristic of a liquid state. A sharp increase of the elastic modulus G' (from 0.15 to 12000 Pa, c.a. 5 orders of magnitude) and viscous G" (from 0.25 to 1700 Pa, c.a. 4 orders of magnitude) moduli was measured between 7h40 min and 15h which quantifies the increase of the viscosity. During this transition, G' becomes higher than G'', suggesting that the elastic behavior becomes predominant. This highlights the formation of a network with a cross-linking density increasing with time. After 15h, the moduli start to decrease, most probably indicating that the sample began to break. In this case, either the applied shear stress was too high or slipping or separation from the plates occurred.

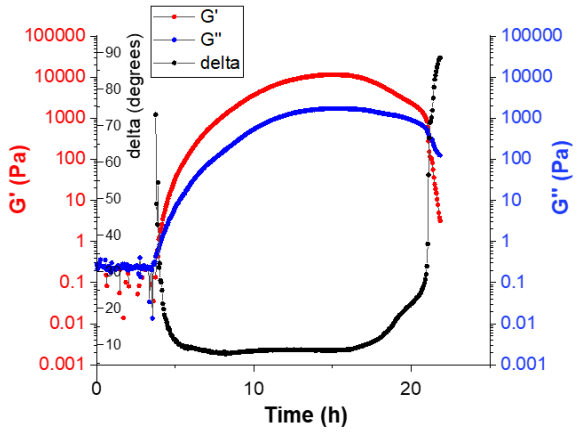

Figure 1: Elastic (G', red), viscous (G", blue) modulus and dephasing (delta, black) of $[Zn(Cy)_2]$/octylamine (OA) mixture over time. The monitoring is started 4 hours after mixing (T= 0 h on the rheogram).

At the end of the experiment, the gap was still adequately filled with a transparent yellowish vitreous solid allowing us to state that the experiment was carried out under conditions that prevented the hydrolysis of the mixture during the measurement. The solid broke up into platelets with the opening of the gap. The rheological data thus demonstrates that the initially liquid mixture became more and more viscous and then starts to behave like a gel or a glassy material. These results are similar to the one already described for the $[Zn(Cy)_2]$/dodecylamine mixture [9] for which rheology and NMR methods gave consistent results: the times at which gelation starts are observed are around 5 and 8h after mixing, respectively.

In the case of hexylamine (see Figure S1), a sharp increase of the moduli is observed at the very beginning of the measurement which does not fit with the results obtained either by NMR or inversion vial test. The change is expected to occur around 20h (13h after injection in the rheometer). The delay between the mixing and the gelation increases when the alkyl chain length of the amine decreases. In the rheometer, the nitrogen flow, even if kept very low, probably flushed out the amine, explaining the abrupt increase of the moduli at the beginning. Besides, small changes during the measurements are observed around 10h and between 23-30h after mixing. The small changes after 23h on the G', G" and dephasing curves fit with the time observed with the two other methods. Despite the sample has clearly not kept the initial proportions, these changes may reflect the changes in the sample viscoelasticity observed with the other methods.

NMR spectroscopic studies: Magic Angle Spinning (MAS) NMR measurements has been carried out for characterization of the pristine $[Zn(Cy)_2]/RNH_2$ mixture as well as to follow on a molecular level the gelation process. Indeed, ^{13}C signal intensities obtained using cross- (CP) and INEPT- polarization transfer sequences yield information on the local dynamics of the alkyl chain: the CP and INEPT sequences edit molecular segments being respectively rigid or mobile [18]. Note that unlike rheology measurements, NMR spectroscopy allows sample preparation and measurement in a controlled atmosphere. The sealed rotors can be prepared in a glove box to protect the reaction medium from humidity. Therefore, measurements are easier to make. This allows the probing of shorter aliphatic chain lengths without changing the stoichiometry of the system being measured. Thus, we not only studied the same mixtures as for the rheology measurements, namely $[Zn(Cy)_2]$/DDA, $[Zn(Cy)_2]$/OA and $[Zn(Cy)_2]$/HA (hexylamine), but we were also able to extend the study to the $[Zn(Cy)_2]$/HPA (heptylamine) system and remarkably also to the system with a chain length as short as pentylamine (PA).

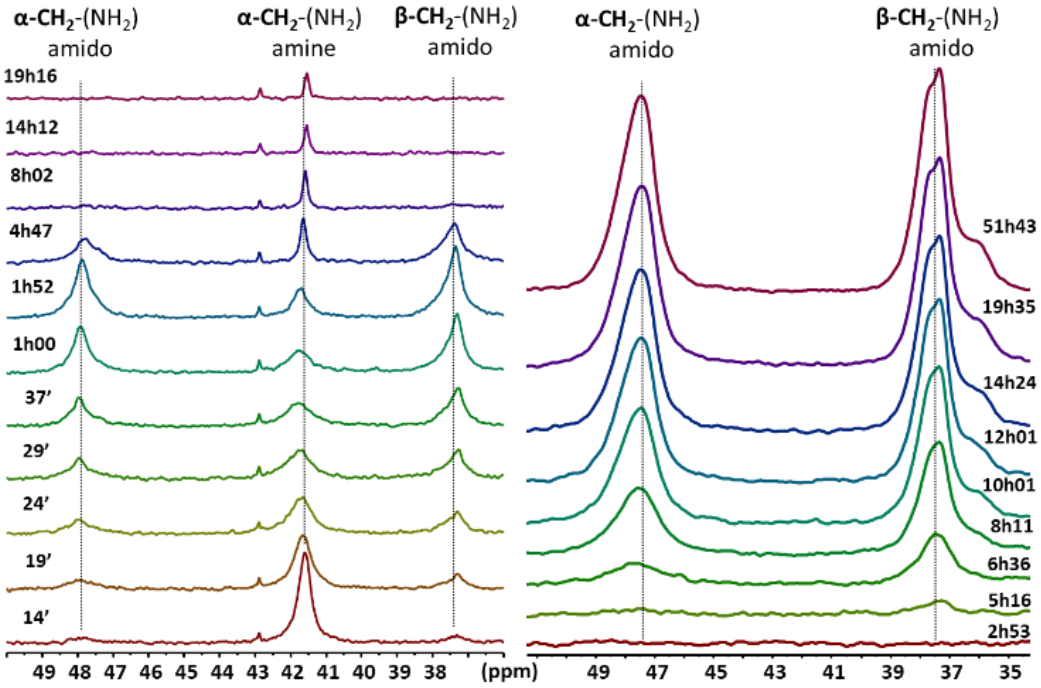

Figure 2: 13C INEPT (left) and CP (right)-MAS experiments of the 34-50 ppm area (full spectra in S3 and S8) of the $[ZnCy_2]$/OA (1:2) mixture over time.

Whatever the length of the alkyl chain may be, there is always a period of time when no signal is detected in the ^{13}C CP-MAS experiments (see Figures 2 right and S2-S6), while strong ^{13}C signals are observed in the ^{13}C INEPT-MAS experiments (Figures 2 left and S7-S11). These results indicate that the $[ZnCy_2]/RNH_2$ mixture starts as a liquid with highly mobile molecules. ^{13}C INEPT-MAS signals characteristic to amine, $[ZnCy_2]$, cyclohexane, and a mixture of monomeric and dimeric Zn amido complexes as well as small Zn amido oligomers are observed (Eq. 3) [9]. Importantly, the intensity of the cyclohexane ^{13}C resonance observed at δ = 26.2 ppm increases over time, indicating the substitution of the Zn coordinated cyclohexyl groups by amido groups. The replacement rate is very similar regardless of the alkyl chain length. Indeed, a plateau is reached after about 8h regardless of the amine (Figure S12).

Additionally, the intensities of the characteristic ^{13}C resonances of the Zn amido species observed at ~47.7 and ~37.3 ppm in the ^{13}C INEPT-MAS spectra begin to increase over time until the signals associated to [ZnCy2] disappear, and then slowly decrease up to their total disappearance. At the end, weak signals of some mobile alkylamine groups can still be detected in the ^{13}C INEPT-MAS, due to the presence of residual amines not involved in the gelation process. Concomitantly, ^{13}C signals of Zn amido oligomers start to appear in the CP-MAS spectra with their intensities increasing over time (Figure 2 (right) and S2-6). These results indicate a rigidification of the alkyl chain of Zn amido oligomers over time. Furthermore, we can note that at the end of the oligomerization, the ^{13}C CP-MAS signal of the carbon close the CH_3 group are weaker than the ones at the center of the alkyl chain or close to the NH group and that the reverse is observed for the ^{13}C INEPT-MAS. These differences are however getting weaker as alkyl chains become smaller. This indicates an increase of the mobility of the methyl group at the alkyl chain extremity for the longest alkyl chains.

Contrary to what has been observed for the substitution rate of the Zn coordinated cyclohexyl groups by amido groups which was very similar regardless of the alkyl chain length, the rates of disappearance of the ^{13}C INEPT signals and of growth of the ^{13}C CP signals associated to the Zn amido species clearly depend on the alkyl chain length. To highlight this effect in a quantitative way, the experimental curves were fitted using a phenomenological model derived from the Finke−Watzky [19] which allows the easy introduction of inhibition phenomena (such as steric hindrance, see SI for details). Table 1 summarizes the average values obtained for each system, namely the induction time ($t_{ind.}$) i.e. the time it takes for the system to start presenting reduced mobility molecules, the time associated to the inflection point (t_{max}) and the associated relative rate (S_{stiff}), i.e. the time required for half of the molecules to have reduced mobility and the instantaneous speed associated with the stiffening phenomenon, and the inhibition time ($t_{inhib.}$) i.e. the time after which the system no longer evolves (see Tables S1 for full values).

Table 1. NMR data

Sample name	S_{stiff} (h^{-1})	t_{max} (h)	t_{ind} (h)	t_{inhib} (h)
$[ZnCy_2]$/DDA	0.19 (0.01)	6.9 (0.4)	5.7 (0.3)	8.0 (0.5)
$[ZnCy_2]$/OA	0.20 (0.01)	6.6 (0.4)	5.4 (0.3)	7.8 (0.5)
$[ZnCy_2]$/HPA	0.02 (0.004)	21.8 (3.0)	13.9 (1.8)	30.0 (4.3)
$[ZnCy_2]$/HA	0.02 (0)	28.7 (3.0)	16.9 (1.4)	40.6 (4.5)
$[ZnCy_2]$/PA	0.01 (0)	114 (1.6)	107.8 (1.8)	120.8 (1.8)

Several type of information can be extracted from these data. Firstly, as the length of the aliphatic chain increases, the gelation time decreases. More precisely, three groups appear. The first group contain the longest alkyl chain length, namely [$ZnCy_2$]/DDA and [$ZnCy_2$]/OA for which the gelation time is around 7h (t_{max}). As the chain length reaches C7 and C6, i.e. for [$ZnCy_2$]/HPA and [$ZnCy_2$]/HA a gelation time between 20 and 30 h is measured. Finally, for the shortest chain length C5, [$ZnCy_2$]/PA system, a significant increase of the gelation time over 100 hours, is observed. Such results indicate, as expected, that van der Walls interactions between the aliphatic chains are involved in the gelation process. Interestingly, when the number of carbons in the alkyl tail is lower than 8, a linear increase of the logarithm of the time parameters is observed versus the number of carbons in the amine backbone (Figure S15). This suggests, for example, that with butylamine (C4) the gelation should theoretically start around 170 h and around 400 h for propylamine (C3).

In addition, for a given chain length, the value of Sstiff is similar whatever the position of the carbon atoms in the alkyl chain (see Table S1). In other words, all the carbon atoms in the alkyl chain have an instantaneous speed associated with t_{max} comparable. It means that as soon as the C atoms start to stiffen, they do so at the same rate. Again, the three groups behave in a similar way but with different orders of magnitude. S_{stiff} is of an order of magnitude larger for the first group containing the longest alkyl chains. Interestingly, the values of t_{max} differ from one carbon atom to another but this variation is similar for the three characteristic times (t_{max}, t_{ind}, and t_{inhib}). In other words, the characteristic time at which the C atoms associated with a signal begin to decrease in mobility, are 50% frozen or completely rigid depends on the position of the C atoms in the aliphatic chain. A more focused look at these results highlights that the order in which the different carbon atoms become rigid is however surprising. The rigidification starts always first on the center of the alkyl chain while it is delayed for the carbons in α- and β- position of the nitrogen and for the terminal methyl groups. These results confirm the presence of strong intermolecular van der Waals interactions between the alkyl chain of the amines but for the first time, it evidences that stiffening of the system takes place first from the aliphatic chains before the inorganic Zn-amido backbone. This remains unexpectedly true up to very short aliphatic chains and makes it possible to distinguish that the driving force of gelation of the system is first the van der Waals interactions, before the oligomerization of the inorganic skeleton by the formation of coordination bonds between the Zn atoms and the nitrogen atoms of the amine group (Scheme 3).

These NMR data demonstrate the effect of time at the molecular level for the formation of the gel and are highly complementary to the rheological experiments which are analyzing the mixtures at the macroscopic level. When the NMR shows the restriction of molecular movements compatible with a gelation process, rheology is the method which really demonstrates that a gel is formed when G' becomes higher than G''.

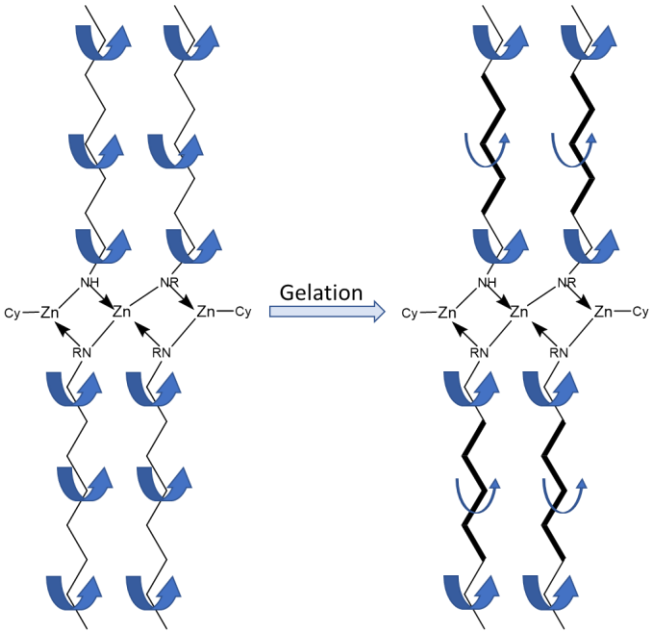

Scheme 3: Proposed mechanism for the formation of the gel.

Conclusion

In this work, we show that the gelation mechanism of the [ZnCy2] organometallic precursor in the presence of primary alkyl amine starts with the rigidification of the aliphatic chains of the amine. This rigidification takes precedence over the oligomerization of the inorganic backbone formed by the acid-base reaction between the zinc organometallic precursor and the alkylamine giving rise to Zn-amido type coordination bonds. Fitting of the experimental data gives quantitative information on this mechanism, key issue to tune the rheological properties of these promising systems.

Experimental Section

Experimental set up for rheology measurement: The elastic modulus (G') and viscous modulus (G'') were monitored with an AR1000 apparatus equipped with an oven (TA Instrument). A flush of nitrogen (0.2 bar) was provided within the oven during the entire experiment. The measurement was made with a 25 mm plate−plate aluminum geometry, and the gap was set at 500 µm. An extra plastic cylinder was placed around the geometry to avoid drying of the sample due to the gas flow. The temperature was 20 °C. The measurements were carried out following the same protocol as described for the $ZnCy_2$/DDA mixture [9]. After the determination of the approximate gelation time by inversion vial tests, a fresh mixture was prepared and left to mature in the glove box up to c.a. 1 hour before the expected transition time. For octylamine: The mixture was prepared in a glove box under argon and stored in a syringe in a Schlenk vial under argon. After 4 h of rest in the syringe, the mixture was injected within the rheometer plate gap (380 µL are injected, the gap between the two plate during injection is set at 1500 µm, the oven is just slightly open to avoid air entrance, the plastic cylinder is lifted during the operation). When the injection is completed, the gap is set at 500 µm, the cylinder is placed so that it does not touch the mobile plate and the oven is closed. The modulus values G' and G'' were measured by applying a sinusoidal stress to the sample, at a frequency of 1 Hz, and the resulting

sinusoidal strain was recorded. Because of the very large change in viscosity during the experiment, the stress applied had to be adapted during the experiment. The stress amplitude is increased 10 folds when the strain decreases below 0.06%. Stress amplitude has been changed this way with small steps to avoid breaking of the structure and separation of the sample from the plates. A stress amplitude of 0.1 Pa was applied from 0 to 6 h of measurement; 1 Pa from 6 to 8.5 h; 10 Pa from 8.5 to 10.75 h; 100 Pa from 10.75 to 22 h.

For hexylamine: The mixture was prepared in a glovebox under argon and stored in a syringe in a Schlenk vial under argon. After 7 h of rest in the syringe, the mixture was injected within the rheometer plate gap. Stress amplitude steps over 50h of the measurement: 0.1/0.5/1/2.5/5/10/25/50/75/100/250/500/750/1000/2500/5000/10000 Pa, with automatic switching when strain < 0.06%.

NMR spectroscopy: Solid-state NMR experiments were recorded at 9.4 T on a Bruker Avance III HD 400 spectrometer. Samples were put into 4 mm zirconia rotors with Kel-F caps that fit perfectly to the rotor inside a glove box. No sign of air contamination was detected. The rotors were spun at 8 kHz at 293 K. π/2 pulses of 2.8 µs and 3.5 µs on ^{1}H and ^{13}C channels were used. Spinal-64 decoupling with a 1H nutation frequency equal to 90 kHz was applied during the acquisition of ^{13}C free-induction decay. ^{13}C with cross-polarisation (CP)-MAS were recorded with a recycle delay of 2 s and a contact time of 2 ms. During the CP transfer, the rf nutation frequency on ^{13}C channel was constant and equal to 60 kHz, whereas the 1H rf nutation frequency was linearly ramped from 40 to 80 kHz. ^{13}C MAS with Insensitive Nuclei Enhanced by Polarization Transfer (INEPT) were recorded with a recycle delay of 3 s, and INEPT delays synchronized with spinning rate of ~1.6 ms and ~1.2 ms (before and after π pulses). The ^{13}C INEPT and CP-MAS spectra were recorded respectively with 80 and 240 scans corresponding to durations of 4’ and 8’. The experimental parameters were optimized in preliminary analyses in order to obtain the best compromise between measurement time and signal to noise ratio. All of the chemical shifts are relative to TMS.

The spectra were apodized with a 10-Hz exponential function. After baseline correction, the area of the signals corresponding to the different carbons (when they can be separated) of the amine were measured by integration with Mnova software. Note that some signals (for example the β-CH_2-(NH_2) amido one in Figure 2) can be composed of several resonances due to the presence of oligomer/polymer of different size and structural heterogeneity.

Acknowledgements

This work was supported by both the Centre National de la Recherche Scientifique (CNRS) and the China Scholarship Council (CSC).

Keywords

gels • rheology • NMR spectroscopy • nanomaterials • organometallic chemistry

References

[1] Nanoparticles: From Theory to Application, Wiley Vch, 2006

[2] a) L. Wang, Z. L. Wang, Nano Today 2021, 37, 101108; b) A. Amiri, R. Shahbazian-Yassar, J. Mater. Chem. A, 2021, 9, 782-823; c) G. Saianand, P. Sonar, G. J. Wilson, A.-L. Gopalan, V. A. L. Roy, G. E. Unni, K. M. Reza, B. Bahrami, K. Venkatramanan, Q. Qiao, J. Energy Chem. 2021, 54, 151–173; d) G. Wang, M. Yu, X. Feng, Chem. Soc. Rev. 2021, 50, 2388-2443; e) S. Arya, P. Mahajan, S. Mahajan, A. Khosla, R. Datt, V. Gupta, S.-J. Young, S. K. Oruganti, ECS J Solid State Sci Technol 2021, 10, 023002.

[3] a) A. Feinle, M. S. Elsaesser, N. Hüsing, Chem. Soc. Rev. 2016, 45, 3377-3399; b) D. Gu, F. Schüth, Chem. Soc. Rev. 2014, 43, 313-344; c) R. Sui, P. A. Charpentier, R. A. Marriott, Nanomaterials 2021, 11, 1686.

[4] a) M. Poddighe, P. Innocenzi, Materials 2021, 14, 6799; b) B. R. Gomes, R. Araújo, T. Sousa, R. B. Figueira, Coatings 2021, 11, 1245.

[5] M. P. Pechini 1967 US3330697 A.

[6] R. Deshmukh, M. Niederberger, Chem. Eur. J. 2017, 23, 8542-8570.

[7] R. Deshmukh, M. Niederberger in Vol. 1 (Ed. M. Z. D. Levy), Wiley-VCH, Weinheim, 2015.

[8] a) G. Garnweitner, M. Niederberger, J. Mater. Chem. 2008, 18, 1171-1182; b) I. Olliges-Stadler, M. D. Rossell, M. Niederberger, Small 2010, 6, 960-966; c) I. Djerdj, M. Cao, X. Rocquefelte, R. Černý, Z. Jagličić, D. Arčon, A. Potočnik, F. Gozzo, M. Niederberger, Chem. Mater. 2009, 21, 3356-3369; d) N. Pinna, J. Mater. Chem. 2007, 17, 2769-2774.

[9] Z. Zhao, Y. Coppel, J. Fitremann, P. Fau, C. Roux, C. Lepetit, P. Lecante, J.-D. Marty, C. Mingotaud, M. L. Kahn, Chem. Mater. 2018, 30, 8959-8967.

[10] a) P. Dastidar, S. Ganguly, K. Sarkar, Chem.: Asian J., 2016, 11, 2484–2498; b) J. K. Wychowaniec, H. Saini, B. Scheibe, D. P. Dubal, A. Schneemann, K. Jayaramulu, Chem. Soc. Rev., 2022, 51, 9068–9126.

[11] S. Mondal, N. Alam, S. Sahoo, D. A Sarma, J. Colloid Interface Sci., 2023, 633, 441–452.

[12] a) N. Malviya, C. Sonkar, B. K. Kundu, S. Mukhopadhyay, Langmuir, 2018, 34, 11575–11585

[13] E. Saha, G. R. Bhadu, J. Mitra, Inter. J. Hydrog. Energy, 2023, 48, 8115–8126.

[14] a) S. Dhibar, H. Dahiya, K. Karmakar, S. Kundu, S. Bhattacharjee, G. C. Nayak, P. Karmakar, G. D. Sharma, B.Saha, J. Mol. Liq., 2023, 370, 121020; b) A. Dey, S. Sil, S. Majumdar, R. Sahu, M. Ghosh, G. Lepcha, P. P. Ray, B. Dey, J. Phys. Chem. Solids, 2022, 160, 110300.

[15] Z. Zheng, R. Butynska, C. Valverde Serrano, J.-D. Marty, C. Mingotaud, M. L. Kahn, Chem. Eur. J., 2016, 22, 15614-15618.

[16] a) S. Saliba, C. Valverde-Serrano, J. Keilitz, M. L. Kahn, C. Mingotaud, R. Haag, J.-D. Marty, Chem. Mater., 2010, 22, 6301; b) Y. Whang, Z. Zhao, Y. Coppel, C. Lepetit, C. Mingotaud, M. L. Kahn, Nanoscale Advances 2021, 3, 6088 – 6099

[17] a) C. E. Hughes, P. A. Williams, K. D. M. Harris, Angew. Chem. Int. Ed. 2014, 53, 8939–8943; b) I. I. Ivanova, Y. G. Kolyagin, Chem. Eur. J. 2021, 27, 14143; c) M. Juramy, G. Mollica, Curr. Opin. Colloid Interface Sci., 2023, 63, 101663.

[18] A. Nowacka, P. C. Mohr, J. Norrman, R. W. Martin, D. Topgaard, Langmuir 2010, 26, 16848-16856.

[19] L. Bentea, M. A. Watzky, R. G. Finke, J. Phys. Chem. C 2017, 121, 5302-53121.

Entry for the Table of Contents

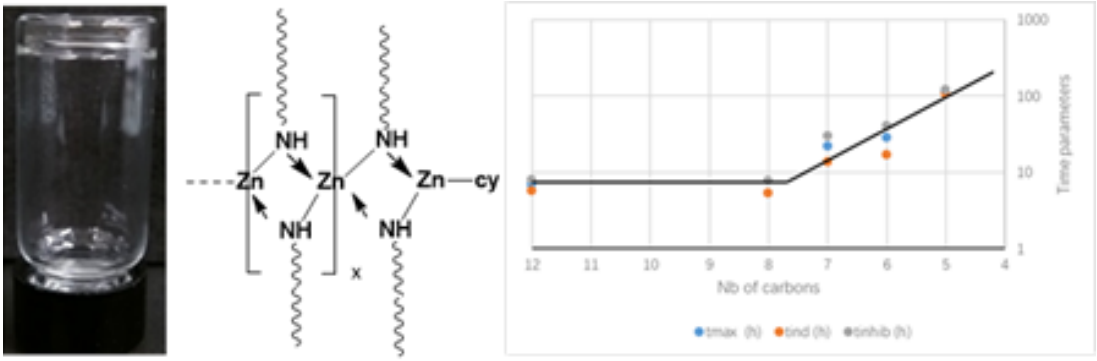

Rigidification of the aliphatic chain takes precedence over the oligomerization of the inorganic backbone. The aliphatic chain length of the amine governs the gelation time.